Comprehensive Comparison of Isolated High Step-up DC-DC Converters for Low Power Application

SAEED POURJAFAR [1] (Member, IEEE), **HOSSEIN AFSHARI** [1] (Student Member, IEEE),
PARHAM MOHSENI[1] (Student Member, IEEE), **OLEKSANDR HUSEV** [1] (Senior Member, IEEE),
OLEKSANDR MATIUSHKIN [2] (Member, IEEE), **AND NOMAN SHABBIR**[1] (Senior Member, IEEE)

[1]Tallinn University of Technology, 12616 Tallinn, Estonia
[2]Tallinn University of Technology and University of Extremadura, 06006 Badajoz, Spain

CORRESPONDING AUTHOR: SAEED POURJAFAR (e-mail: sapour@taltech.ee).

ABSTRACT In this paper comprehensive evaluations of isolated high step-up dc-dc topologies have been investigated. These converters are especially well suited for distributed generation systems utilizing renewable or alternative energy sources that need a wide input voltage range with load regulation. With this in mind, this work primarily concentrates on comparative analysis of various isolated configurations employed in possible industry applications. Consequently, several isolated structures, including flyback, forward, push-pull, and full bridge and other similar solutions have been carried out in the literature. For the purpose of comparative and theoretical analysis, some of the circuit parameters are considered, which include voltage conversion ratio, semiconductor element voltage stress, component size, and conduction and switching losses. Furthermore, the selected configurations have been discussed in terms of cost estimation and financial feasibility. In addition, the design procedure and experimental prototypes of the available solutions with the main results are presented. Derived from this investigation, the authors provide a guide to help researchers to identify different isolated topologies with wide input voltage range and galvanic isolation for prospective research directions within this area.

INDEX TERMS Isolated high step-up converter, distributed generation systems, wide input voltage range.

I. INTRODUCTION

Environmental concerns, including issues like global warming, the limited availability of fossil fuels, and the need to decrease carbon dioxide emissions, have motivated the research for cleaner and more sustainable energy sources [1]. Simultaneously, there has been a growing demand for renewable energy systems such as solar panels, fuel cells, and wind turbines in recent years. This increased demand for cleaner energy options has led to a shift in thinking about operating grid-connected systems, necessitating the development of innovative strategies [2], [3]. In essence, the challenges posed by environmental issues and the push for renewable energy are reshaping the energy landscape and how power is generated and distributed [4], [5].

In recent times, microgrids have gained considerable attention due to the substantial benefits they offer to both electricity consumers and power grid operators. Microgrid deployments are seen as a means to enhance power quality, lower emissions, ease network congestion, reduce power losses, improve energy efficiency, and potentially enhance the overall economic performance of the system [6]. Furthermore, over the past decade, dc microgrids have garnered significant interest from both academia and industry. These dc microgrids have proven to be superior to ac microgrids in terms of reliability, efficiency, ease of control, integration of renewable energy sources, and connecting dc loads [7]. The architecture of a simple dc microgrid with a various power conversion section is depicted in Fig. 1.
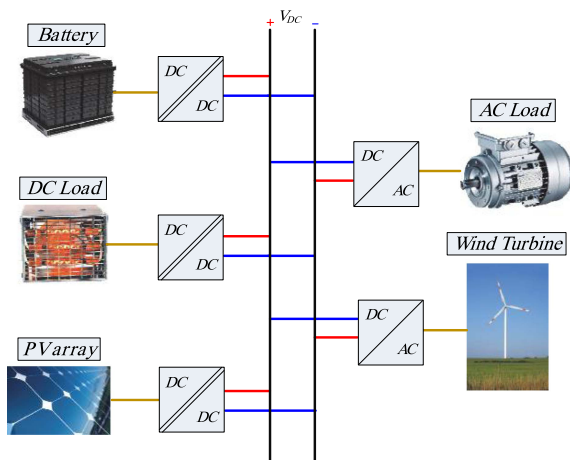
FIGURE. 1. A simple architecture of DC Microgrid.

TABLE 1. Main Features Comparison of VF, CI and IS Converters

Feature	VF	CF	IS
Voltage step-up	No	Yes	Yes
Voltage step-down	Yes	No	Yes
Short-circuit exemption	No	Yes	Yes
Open-circuit exemption	Yes	No	Yes
Element for storing energy	One capacitor	One inductor	At a minimum, one capacitor and one inductor.
Cascading capability of energy elements	No	No	Yes
Simplicity in control	Simple	Complex	Moderate

The primary challenge in implementing a dc grid is the lack of a viable business model. Hence, the power electronic converters need to be versatile and compatible with both dc and ac applications [8], [9]. Power electronic structures play a crucial role in incorporating renewable energy generation into the power grid, meanwhile their usage is widespread and expanding rapidly [10].

Solar Photovoltaic (PV) energy is a highly significant global energy source and is projected to be the leading contributor to electricity generation among all renewable options by 2040. This is due to its renewable nature, absence of harmful emissions, and high efficiency. PV power plants are an effective means of harnessing energy from the sun and directly converting it into electricity [11] and [12]. However, PV panels produce very low voltage, and for applications requiring high voltage, these panels must be connected in series and parallel configurations. Unfortunately, this approach increases the overall cost of PV power systems. To address the issue of low voltage output from PV panels, a high step-up dc-dc converter is needed to boost the low voltages (typically 20–30 V) to align with the voltage level for distribution of a dc microgrid (usually 350–400 V) [13], [14].

Lately, there have been numerous advancements in high step-up dc-dc converters designed to achieve high voltage gains in both isolated and non-isolated configurations [15], [16]. In non-isolated setups, where galvanic isolation is not present, various methods have been employed to enhance the dc-dc conversion process. These methods include using coupled inductors, cascading techniques, switched capacitors, switched inductors, and voltage multiplier cells [17]. They are used to achieve a substantial voltage boost in a cascade setup without the need for a transformer, all while maintaining high efficiency and high-power density [18]. To link energy sources with lower input voltages to a higher-voltage dc bus, galvanically isolated dc-dc converters are among the most promising solutions.

These converters provide isolation to shield the energy source from significant voltage fluctuations at the load. They

are efficient in utilizing the energy source, offer more flexibility in handling varying load conditions, and are capable of working with a wider range of input voltages [19], [20], [21], [22], [23]. Various established isolated dc-dc converters can be broadly categorized as Voltage-Fed (VF) and Current-Fed (CF) converters. Current-fed converters primarily function by reducing the input voltage through the adjustment of switch duty cycles [24], [25]. They typically incorporate an output LC filter, which smoothens the pulsating voltage. To operate as boost isolated dc-dc converters, current-fed dc-dc converters offer several advantages, including reduced input current ripple, a lower transformer turns ratio, improved efficiency, lower voltage requirements for rectifier diodes, and the absence of shoot-through faults in power switches [26]. Moreover, there is another isolated converter called Impedance Source (IS) converter, which is a combination of VF and CF converters, and it can have the characteristics of both of them [19], [27], [28], [29]. To better understanding, the specifications of these three types of converters been compared with each other and illustrated in Table 1 [30]. Alternatively, in different scenarios, isolated converters can be classified into three primary types: those based on full or half-bridge switching (BS), single or two-switch PWM, and resonant designs. Full-BS converters offer high voltage step-up ratios and efficiency but are better suited for high-power applications due to their numerous switches [31]. For low-power applications PWM, half-BS, and resonant converters are more practical [32]. In PWM DC-DC converters, standard configurations such as Cuk, SEPIC, and Zeta, incorporating galvanic isolation, as well as Forward, Flyback, and Push-Pull designs, are simple yet may exhibit certain constraints such as reduced static voltage step-up ratios, high input current ripple, and the need for high-breakdown voltage diodes [33]. Isolated High step-up dc-dc converters also can be divided into two types: passive clamp and active clamp converters.

Passive clamp converters have a simple structure and few switches but suffer from power losses due to hard switching of the main switch [34]. Active clamp converters, based on push-pull, half-bridge, and full-bridge topologies, achieve zero-voltage switching (ZVS) for switch turn-on and eliminate voltage spikes. However, they may not be highly efficient or cost-effective in low-power applications due to increased switch count and complex driving circuits [35].

Resonant bridge isolated high step-up dc-dc converters address issues with soft switching, using parasitic elements for resonance and featuring a simple structure without clamp circuits. However, they may cause a significant dc-offset current in the transformer, increasing its size [36].

This paper presents a comprehensive evaluation of isolated high step-up DC-DC converter topologies for distributed generation systems using renewable energy sources. Unlike existing reviews that focus on individual converter types, this paper conducts a thorough comparative analysis across multiple configurations, including flyback, forward, push-pull, and full-bridge converters. The evaluation considers critical parameters such as capacitor and magnetic sizes, primary side switch voltage stress, semiconductor conduction losses, and switching losses, standardized for a fair comparison under identical conditions of 400 W output power, 20–50 V input voltage range, and 50 kHz switching frequency, maintaining a constant 350 V output voltage. The main contributions of the paper include:

1) *Component Sizing Analysis:* Introducing a quantitative approach to compare capacitor and magnetic sizes based on accumulated energy calculations, aiding in optimizing component selection.

2) *Voltage Stress and Losses Comparison:* Utilizing normalized parameters like Voltage Stress Ratio (VSR) and Conduction Loss Ratio (CLR) to evaluate primary side switch voltage stress and semiconductor conduction losses.

3) *Switching Losses Assessment:* Employing a Switching Loss Ratio (SLR) to assess the efficiency of switching losses management across different converter types.

To validate the comparative methodology, a series of experiments were conducted under controlled laboratory conditions. Representative converters, one using coupled inductors (flyback) and another using a transformer (full-bridge), were selected for direct performance comparison. This setup ensured a fair and equitable comparison of efficiency, losses, thermal characteristics, and cost-effectiveness under similar operating conditions.

By evaluating key performance indicators crucial for real-world applications, such as efficiency under varying loads, detailed losses analysis, thermal behavior, and cost considerations, this paper provides practical insights into the strengths and weaknesses of each converter type. Unlike many theoretical studies, this paper bridges theory with practice by incorporating experimental validation. The classification of converters into coupled inductor-based and transformer-based categories, based on their operational principles, aligns with the distinctions made in the introduction and the main body of the paper. This classification is essential for understanding the different converter types and their applications in renewable energy systems. The paper is structured as follows:

1) Section II provides an overview of the competitive solutions.

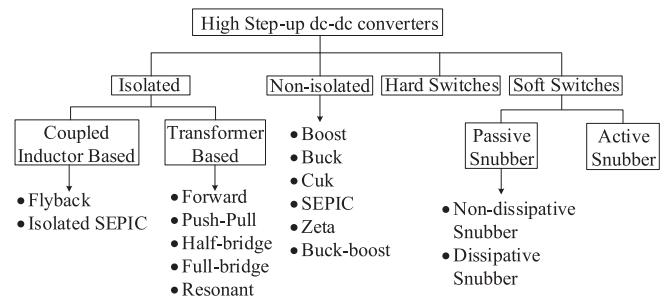2) Section III delves into the methodology for comparative evaluation and offers guidelines for component design.

FIGURE. 2. Classification of high step-up DC-DC converters.

3) Section IV offers experimental evaluation of the proposed solutions.

4) Finally, Section V presents the conclusions drawn from this study.

Overall, this paper aims to guide engineers and researchers in selecting optimal DC-DC converter topologies for diverse renewable energy applications, contributing significantly to the field by combining theoretical insights with practical validation.

II. OVERVIEW OF COMPETITIVE SOLUTIONS

The concise summary of the categorization of high step-up DC-DC converters for both isolated and non-isolated types is illustrated in Fig. 2. This paper primarily concentrates on isolated dc-dc converter topologies. Several isolated high step-up dc-dc converters have gained prominence in the industry due to their efficiency, capability, and suitability for applications such as single-phase PV application. The conventional isolated converters, as shown in Fig. 2, include coupled-inductor based converters like Flyback, isolated SEPIC, and transformer-based converters consisting of various topologies such as forward, Push-pull, voltage-fed half-bridge, voltage-fed full-bridge, current-fed half-bridge, current-fed full-bridge, resonant half-bridge, and resonant full-bridge. These converters are widely used based on their inherent characteristics, performance metrics, and suitability for specific applications. Table 2 provides a concise merits and demerits of main features among the conventional isolated high step-up dc-dc converters. In next sub-sections, a set of these solutions has been explained and discussed.

A. COUPLED INDUCTOR BASED ISOLATED SOLUTIONS

The isolated SEPIC, is one of the coupled inductor based isolated converter, commonly used in renewable application, which has advantages like low-input current ripples, minimal EMI, and versatile outputs. These converters possess a fundamental flaw, experiencing notable voltage stress on switch devices that is on par with the combined magnitude of both output and input voltages [37], [38], [39].

Flyback based converter, with its coupled-inductor based isolation, is known for its simplicity and cost-effectiveness. It is suitable for low to moderate power applications [40],
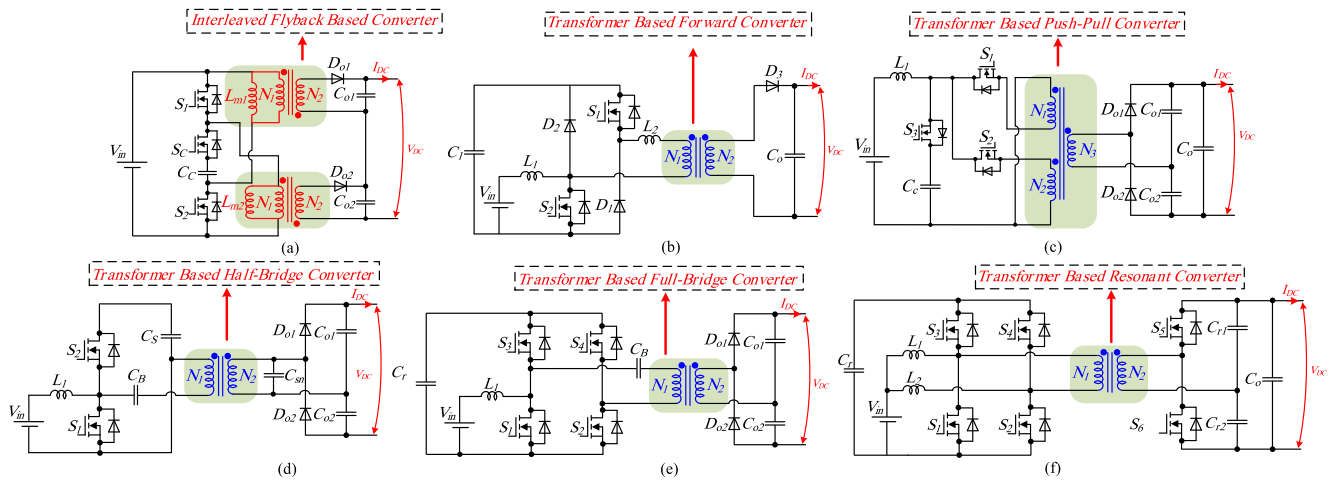
FIGURE. 3. Several isolated high step-up DC-DC converters for dc-microgrid applications, (a) Flyback based converter [47], (b) Forward based converter [52], (c) Push-pull based converter [54], (d) Half-bridge based converter [56], (e) Current-fed FB with clamp capacitor [58], and (f) Current-fed resonant converter [67].

TABLE 2. Comparison of Conventional Isolated Converters

Topology	Advantages	Disadvantages
Flyback	• Simple design and low cost. • Suitable for low to moderate power applications	• Limited power handling capability • High peak currents and voltage stresses
Isolated SEPIC	• Dual voltage regulation: step-up and step-down capabilities. • Reduced input current ripple	• Complex control and higher component count • Limited for high power applications.
Forward	• High efficiency • Good for high power applications	• Limited voltage regulation range. • Requires tight control for reliable operation
Push-pull	• High-frequency operation capability • Good for high power applications.	• Complex control and higher component count • Transformer design can be challenging
Half-bridge	• Moderate complexity. • Suitable for a wide range of power applications.	• Requires careful control to avoid voltage spikes • Limited for very low or very high power
Full-bridge	• High efficiency. • Suitable for high-power applications	• Complex control and higher component count • Not ideal for low-power applications.
Resonant	• Reduced electromagnetic interference (EMI) • Improved reliability due to soft switching	• Complex control and higher cost • High current stress through the semiconductor devices

[41], [42], [43], [44], [45]. The conventional flyback converter topology has drawbacks that limit its performance in some applications. Some issues include high voltage spikes and oscillations caused by leakage inductance in the main transformer, reducing efficiency and risking switch and diode damage. Furthermore, the main switch requires a high voltage rating due to the summation of input and reflected output voltages [46]. Fig. 3(a) depicts a two-switch flyback PWM dc–dc converter with active snubber [47]. The proposed converter introduces a dual-flyback high step-up, enhancing voltage gain while minimizing turn ratios. Increasing voltage gain and

reducing switching losses are achieved by coupling two series secondary inductors.

To minimize input current ripple, the two primary sides are interconnected in a parallel configuration.

B. TRANSFORMER BASED ISOLATED SOLUTIONS
The forward converter is one of transformer based isolated solutions that extensively employed in applications requiring low to medium power supplies, primarily owing to its straightforward design and cost-effectiveness. Nonetheless, it possesses two primary disadvantages: When the switch is deactivated, the energy confined in the magnetizing inductance within the core results in transformer saturation, and the transformer's leakage inductance subjects the switch to substantial voltage stress [48], [49], [50], [51]. Ref. [52] introduces an innovative Active-Clamp Forward Converter (ACFC) incorporating a lossless snubber on the secondary side to mitigate voltage spikes on the free-wheeling diode and forward-rectifier diode. Fig. 3(b) depicts the circuit configuration of the suggested converter.

The Push-Pull based converter is other transformer based isolated solution, which utilized in single phase PV applications. This converter is known for its simplicity and reduced component count, is often chosen for applications where isolation and high step-up ratios are essential. While cost-effective and efficient, it may face challenges in EMI [53]. One push pull based converter with Three Winding Transformer (3WT) has been illustrated in Fig. 3(c) [54]. This configuration's primary benefit lies in its capacity for achieving a high voltage gain, operating with ZVS, and offering a wide operational range suitable for applications like PV microconverters.

A half-bridge converter finds wide application in motor drives, power supplies, battery chargers, and renewable energy systems. Similar to forward and push-pull converters, it can generate variable output voltages and offer electrical isolation. Despite its more intricate design compared to

forward or push-pull converters, the half-bridge converter delivers greater output power using fewer and cost-effective components [55]. Ref. [56] (Fig. 3(d)) explored an efficient quasi-resonant boost half-bridge dc–dc converter for PV micro-inverters, with a wide input voltage range. The design optimized conversion using a voltage doubler and snubber capacitor, eliminating DC-magnetizing currents in transformers. Employing quasi-resonance in switches and diodes achieved ZVS, minimizing turn-off losses.

The isolated Full-Bridge (FB) converters, which is another transformer based solution, offers improved efficiency and reduced stress on components compared to its half-bridge counterpart. Its full-bridge configuration allows bidirectional power flow, making it suitable for applications demanding higher power density [57]. In [58], which demonstrated in Fig. 3(e), a current fed FB with wide input voltage range has been presented. The voltage spike throughout this converter has been decreased because of using clamp capacitor.

Resonant converters, notably the LLC type, are gaining attention for their outstanding performance [59], [60], [61], [62], [63], [64]. Their benefits and drawbacks vary based on application needs like power density, efficiency, cost, complexity, and reliability [65]. The LLC converter, with low EMI, high power density, and ZVS capability in switches, is particularly favored. In high-step-up PV applications, LLC resonant converters operating at resonant frequencies are preferred for efficient power conversion [66]. Nevertheless, integrating additional components leads to increased magnetic loss, costs, and complexity within these converters. In [67] (Fig. 3(f)), a resonant dc-dc converter was created with the aim of attaining input currents devoid of ripples. Through the maintenance of a consistent duty cycle and the incorporation of a resonant circuit on the secondary side, this converter reduces turn-off currents and minimizes switching losses, ultimately enhancing efficiency.

III. COMPARISON METHODOLOGY OF ISOLATED SOLUTIONS

In this section, a comprehensive comparison of solutions depicted in Fig. 2 is conducted using a methodology that considers key parameters such as follows:

1) Capacitor size
2) Magnetic size
3) Primary side switch voltage stress
4) Primary side semiconductor conduction losses
5) Switching losses

The design parameter of comparison for all converters has been indicated in Table 3.

Capacitor size impacts energy efficiency, inductor size influences energy transfer, and high frequency transformer dimensions, which are magnetic elements, affect overall system size and efficiency. Analysis of relative conduction and switching losses of semiconductors provides insights into system efficiency and control mechanisms. Additionally, evaluating primary side switch voltage stress informs about component reliability. In a very general case, the fundamental

TABLE 3. Design Parameter of Comparison for All Converters

Parameters	Value
Input voltage range (V_{in})	20 V – 60 V
Output voltage (V_o)	350 V
Maximum rated power (P_o)	400 W
Switching frequency	50 kHz
Maximum input current	10 A
Maximum input current ripple	15 %
Maximum voltage ripple of capacitors	3 %

waveforms of a converter are independent of the selection of components and electric parameters (e.g., switching frequency, selected semiconductors) and result from the basic modulation scheme, yielding some general requirements for the dimensioning of the components [68]. This approach offers a nuanced understanding of the strengths and weaknesses of each solution, aiding engineers and researchers in optimizing these converters for diverse applications. It was applied in some other research works [69], [70].

A. MAGNETIC AND CAPACITORS SIZE COMPARISON

For comparing capacitor and magnetic sizes among the solutions, a methodology relies on calculating the total accumulated energy in these elements. This quantitative approach evaluates their energy storage capacities, providing insights into efficiency. The analysis also considers total conduction power loss, offering a holistic perspective on how effectively each solution manages power flow through these components. Therefore, the following equations has been utilized:

$$\sum_{i=1}^{n} E_{C_i} = \frac{1}{2} C_i V_{C_i}{}^2, \tag{1}$$

$$\sum_{j=1}^{m} E_{L_j} = \frac{1}{2} L_j I_{L_j}{}^2. \tag{2}$$

In the above equations, E_C, E_L, V_C, I_L, n and m are respectively the accumulated energy in capacitors and inductors, the voltage across the capacitors, the current through the inductors, number of capacitors and number of inductors.

B. PRIMARY SIDE SWITCH VOLTAGE STRESS COMPARISON

To compare the primary side switch voltage stress (V_{stress}) of switches, a normalized parameter called the Voltage Stress Ratio (VSR) can be used as follows:

$$VSR = \frac{V_{stress}}{V_{out}}. \tag{3}$$

This ratio provides a comparative measure that considers the impact of the voltage stress relative to the output voltage. A lower VSR indicates that the primary side switch voltage stress is a smaller proportion of the output voltage, which can be useful for evaluating the stress level on the switch in relation to the desired output voltage.

C. PRIMARY SIDE SEMICONDUCTOR CONDUCTION LOSSES COMPARISON

The primary side semiconductor conduction losses in mentioned converters are compared based on normalized parameter known as the Conduction Loss Ratio (CLR). The CLR is expressed as the ratio of the conduction losses to the total power:

$$CLR = \frac{P_{Condcution}}{P_{out}}. \tag{4}$$

In (4) P_{out} is the total power of the converter and $P_{conduction}$ represents the total conduction losses in the primary side semiconductor devices that define as follows:

$$P_{conduction} = \sum_{i=1}^{N} R_{on}I_{RMSi}^2. \tag{5}$$

I_{RMS} is the Root Mean Square (RMS) current flowing through the semiconductor device during conduction, and R_{on} is the ON-state resistance of the semiconductor device.

D. SWITCHING LOSSES COMPARISON

The switching loss ratio (SLR) is defined as the ratio of the switching losses to the total power for this comparison as follows:

$$SLR = \frac{P_{switching}}{P_{out}}. \tag{6}$$

The switching losses ($P_{switching}$) occur during both turn-on and turn-off events are influenced by semiconductor parameters such as the switching frequency, device capacitances that we assume to be similar to all compared solutions, while the voltage and current waveforms during switching are define by the selected topology and are expressed as follows:

$$SL \cong \sum_{i=1}^{N_S} \left\langle \hat{i}_{Si} \cdot \hat{v}_{Si} \right\rangle_T. \tag{7}$$

In (7), the average of the product v_{Si} and i_{Si} throughout a fundamental period T serves as an appropriate indicator for assessing switching losses. Besides, SLR provides a comparative measure for evaluating how efficiently the converter handles switching losses relative to the total power. Based on the mentioned specification for methodology of comparison, the converters presented in Fig. 3 from each family of isolated converter has been compared with each other that is indicated in Fig. 4.

The comparison performance of each converter separately has been illustrated in Fig. 5. It is essential to emphasize that this comparative analysis is specifically implemented with an output power set at 400 W. The input voltage ranges between 20 V and 50 V, with a consistent switching frequency of 50 kHz, while the output voltage is maintained at a constant 350 V. To ensure a comprehensive and fair comparison, not only is the output power standardized, but the duty cycle and other dynamic switch configurations are also kept consistent
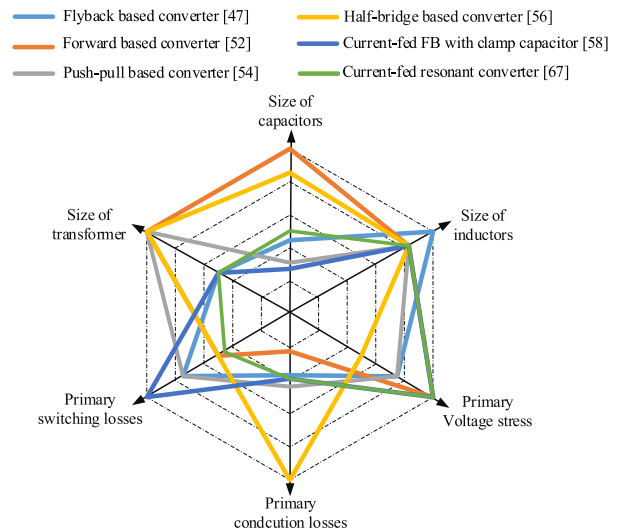

FIGURE. 4. Overall comparison of the isolated converters form each family based on key parameters.

across all converters. It's worth noting that isolated high-step-up converters typically incorporate a voltage multiplier rectifier on their secondary side, a common feature among most isolated converters.

As a result, specifications related to the secondary side, such as the voltage stress of diodes and conduction losses, have been omitted from this comparison. This intentional exclusion allows us to focus specifically on the primary aspects influencing performance, providing a standardized basis for evaluating the efficiency and effectiveness of the converters. This meticulous approach ensures that the comparison is not only fair but also comprehensive, enabling a detailed examination of the converters' performance under consistent conditions.

In general isolated converters have been extensively employed across different power levels, frequently as adaptations of non-isolated converters [71] and [72]. As previously noted, DC-DC converters featuring galvanic isolation can be classified based on the energy transmission element as either transformers or coupled inductors [26]. Even though both transformers and coupled inductors share the commonality of having multiple windings on a magnetic core, their operational principles and roles in switching converters exhibit significant variations [73]. Transformers are the favored option for achieving galvanic isolation due to their noteworthy power density, making them a popular choice for high-power applications. Conversely, converters based on coupled inductors present a more efficient solution characterized by a smaller size and weight. Moreover, they find common use in applications with lower power requirements [74].

IV. EXPERIMENTAL EXAMPLE OF ISOLATED DC-DC CONVERTERS

To validate the comparison methodology, a series of experiments with various configurations was conducted in the
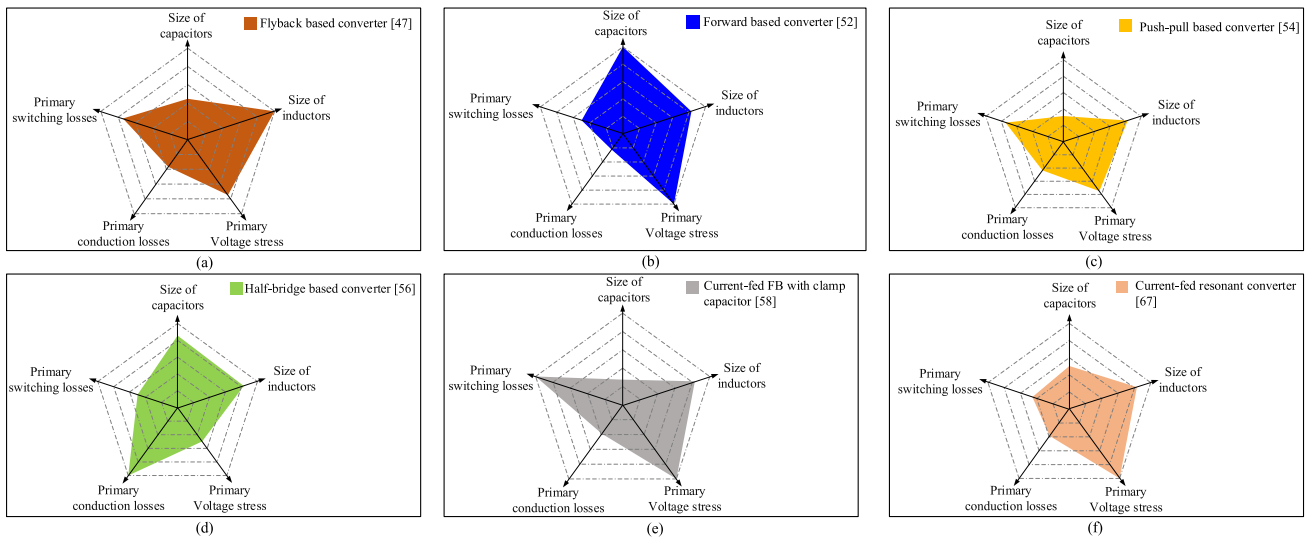
FIGURE. 5. Performance Comparison of the isolated converters, (a) Flyback based converter [47], (b) Forward based converter [52], (c) Push-pull based converter [54], (d) Half-bridge based converter [56], (e) Current-fed FB with clamp capacitor [58], and (f) Current-fed resonant converter [67].
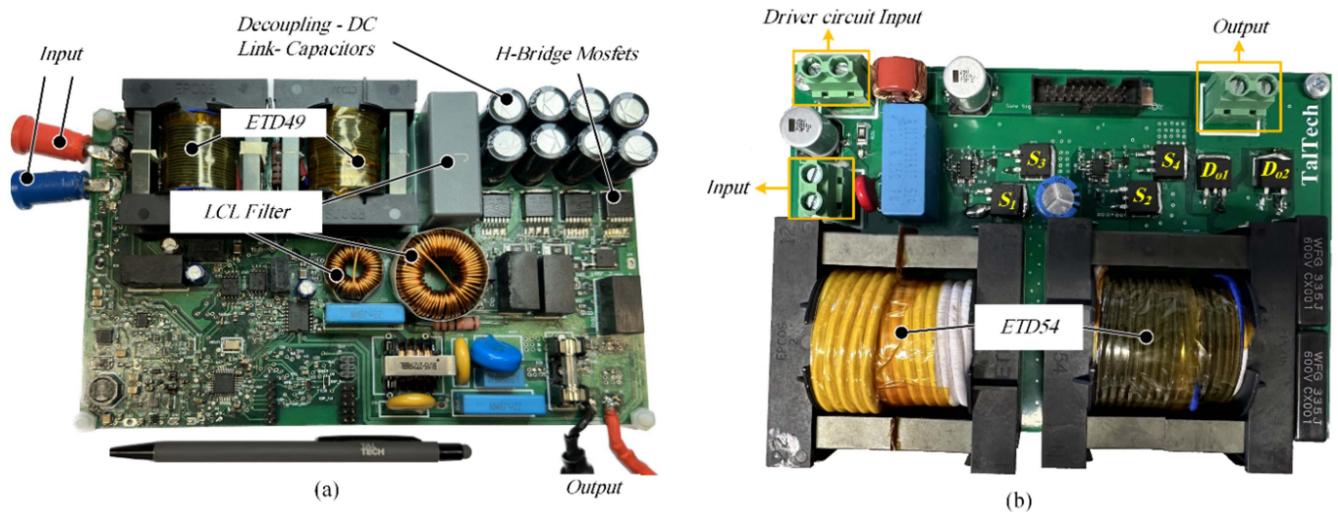

FIGURE. 6. The experimental prototype of the isolated converters, (a) Flyback based converter, (b) FB based converter.

laboratory. In this specific comparison, the flyback converter was chosen from the family of isolated converters due to its reliance on the coupling inductor. Similarly, the full-bridge converter, selected from the same family of isolated converters, was chosen based on its use of a transformer. Moreover, Fig. 6 illustrates the experimental prototypes of each converter.

It's crucial to emphasize that the flyback converter showcased in this study was meticulously designed for PV microinverter applications and includes additional components because of its performance [45]. However, for a fair and focused comparison, only the DC portion of the flyback converter was considered. This deliberate choice enables a comprehensive and equitable evaluation of the essential aspects pertinent to the comparison. The parameter specifications for both converters are provided in Table 4. Both converters underwent testing with an input voltage range of 20–60 V and a power rating of 400 W. The experimental waveforms for both the flyback-based high step-up converter and the full-bridge (FB) based converter are presented in Fig. 6. It is crucial to note that these waveforms were obtained with an input voltage fixed at 40 V and a constant output voltage of 350 V. In Fig. 7(a), the waveforms for input voltage (V_{in}), output voltage (V_{out}), and input current of the FB-based converter are displayed. Notably, the input current ripple content is approximately 20 %, indicating an acceptable level for this type of converter. Fig. 7(b) depicts the voltage and current waveforms of the main switches of the FB-based
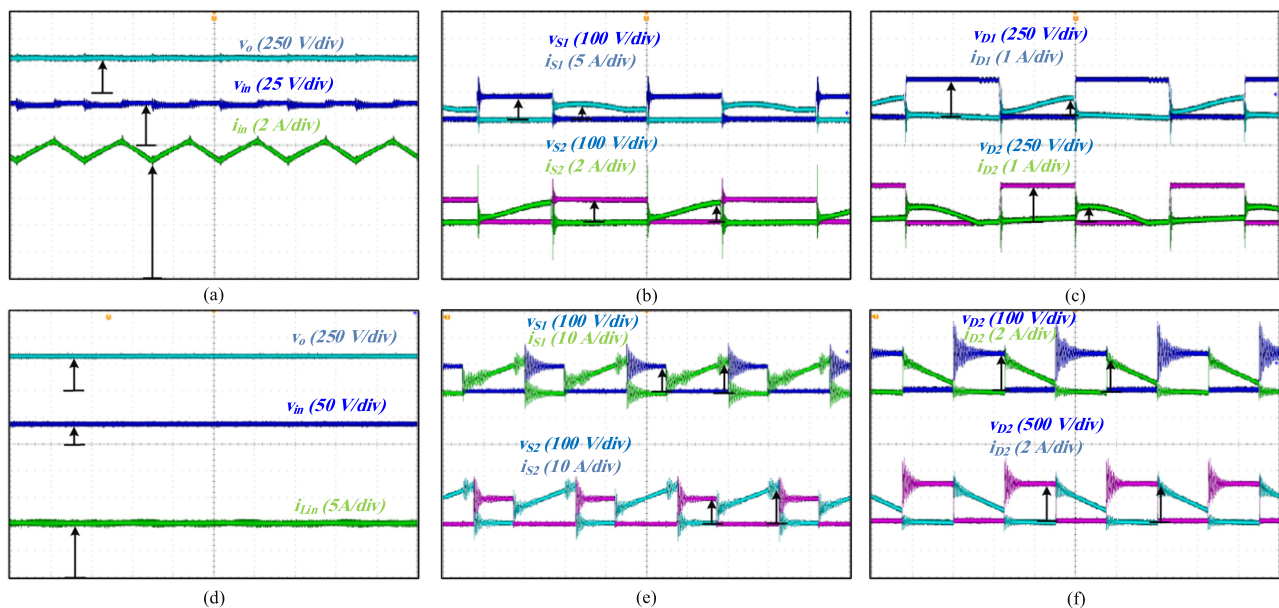
FIGURE. 7. Experimental measurement of the isolated dc-dc converters, (a) Input voltage (V_{in}), output voltage (V_{out}) and input current of FB based converter, (i_{in}) waveforms, (b) current and voltage waveforms of switches S_1 and S_2 of FB based converter, (c) current and voltage waveforms of diode D_1 and D_2 of FB based converter, (d) Input voltage (V_{in}), output voltage (V_{out}) and input current (i_{in}) of flyback based converter, (e) current and voltage waveforms of switches S_1 and S_2 of flyback based converter, (f) current and voltage waveforms diodes D_1 and D_2 of flyback based converter.

**TABLE 4.** Specification of the Isolated Converters

Parameters	Value/Type	
	Flyback based	FB based
Transformer core	ETD49	ETD54
Input inductor	-	220 μH
Magnetic inductance	60 μH	870 μH
Leakage inductance	450 nH	1.7 μH
Decoupling capacitor	8 × 22 μF	-
Capacitors C_b, C_r	-	22 μF, 10 μF
Semiconductor elements		
Switches $S_1..S_4$	-	IPB048N15N5LFATMA1
Diodes D_{o1}, D_{o2}	IDM05G120C5XTMA1	C6D08065G
Flyback switches	IPB044N15N5ATMA1	IPB044N15N5ATMA1
Operating point		
Input voltage range (V_{in})	20 V – 60 V	20 V – 60 V
Output voltage (V_o)	350 V	350 V
Maximum rated power (P_o)	400 W	400 W
Switching frequency	60 kHz	60 kHz

converter. From this figure, it is observed that the voltage stress on the two main switches is around 90 V, which is four times smaller than the output voltage. Moving to Fig. 7(c), the voltage and current waveforms of the voltage multiplier rectifier diodes (D_1 and D_2) are illustrated. The voltage stress on the output diode matches the output voltage, a typical characteristic in converters of this kind. Switching our attention to the isolated flyback converter, Fig. 7(d) showcases the input voltage, output voltage, and magnetizing current waveforms. A comparison with the FB-based converter reveals that the input current ripple of the flyback-based converter is generally higher. In Fig. 7(e), the voltage and current of switches S_1

and S_2 are presented, indicating a maximum switch voltage of around 120 V. In terms of voltage stress evaluation, although each switch's voltage stress in the FB-based converter is lower than that of the flyback-based converter, the total voltage stress in the FB-based converter is higher when compared to the flyback-based converter. Finally, Fig. 7(f) exhibits the voltage and current waveforms of the output diodes, revealing that their voltage stress is twice as high as the output voltage. While this may suggest high stress on the output diodes, it is noteworthy that there are also flyback-based converters mentioned in previous studies [45], where the output diode voltage stress aligns with the output voltage. In summary, the waveforms analysis indicates distinct performance characteristics between the flyback-based high step-up converter and the FB-based converter. The FB-based converter demonstrates lower voltage stress on individual switches but higher total voltage stress. The output diodes in the FB-based converter exhibit higher stress, yet it's important to recognize that similar stress levels have been reported in certain flyback-based converters according to prior studies [45]. Choosing between the two converters depends on the specific application requirements and observed waveform characteristics

In order to provide a thorough comparison between coupled inductor-based and transformer-based structures, various key performance aspects have been analyzed and presented in Fig. 8(a)–(e) for both converters. These figures offer insights into the efficiency curve, losses breakdown of the power circuit, and thermal characteristics of the main switches for both FB based and flyback based converters.

In Fig. 8(a), the efficiency curve shows the performance of the proposed converters across a range of output power

(a)
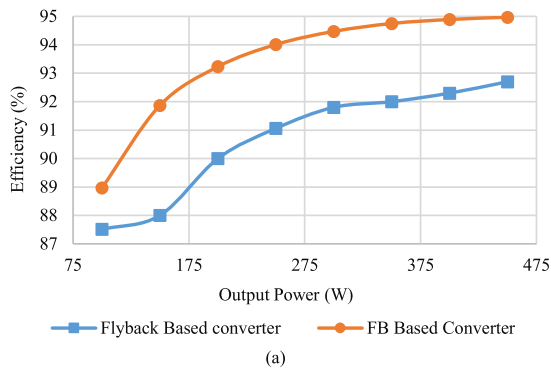
Power Losses Breakdown of FB Based Converter

(b)
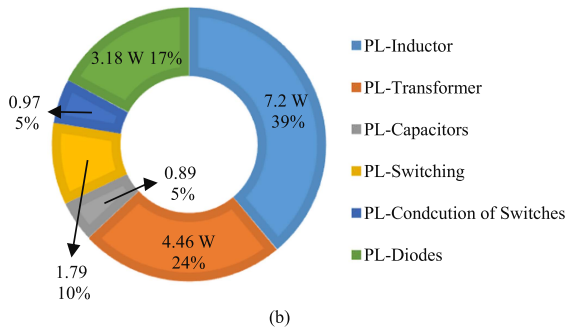
Power Losses Breakdown of Flyback Based Converter

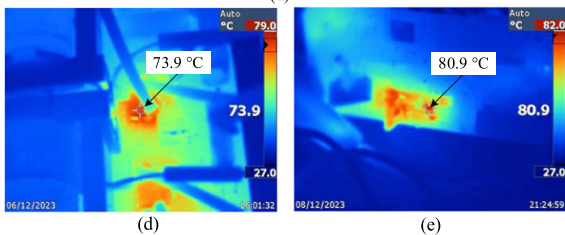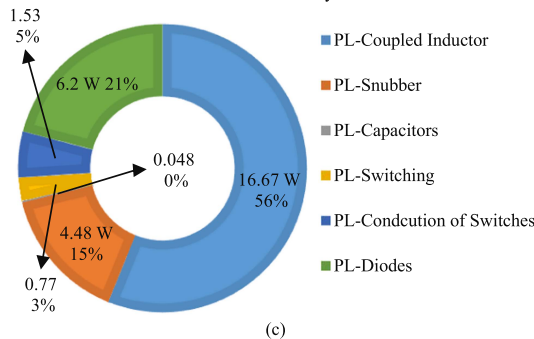(c)

(d)   (e)

FIGURE. 8. Efficiency, power loss curve and thermal image flyback based and FB based converters, (a) Efficiency curve versus output power, (b) Total losses breakdown of the components in FB based converter, (c) Total losses breakdown of the components in flyback based converter, (d) Thermal image of the main switch in FB based converter, (e) Thermal image of the main switch in flyback based converter.

FIGURE. 9. The cost graph of the image flyback based and FB based converters for different numbers of assemblies.

This commonality underscores the intrinsic nature of losses associated with these components. Notably, the Flyback converter introduces additional losses in the form of snubber circuit losses, which are conspicuously significant.

This observation raises considerations for optimizing the snubber circuit design to mitigate its impact on overall efficiency. Furthermore, the temperature curves of the main switches for each converter, as depicted in Fig. 8(d) and (e), highlight the thermal characteristics under the specified operating conditions. Based on this Figs, both converters demonstrate satisfactory thermal performance in this scenario, indicating that neither converter is adversely affected by excessive heating issues. In Fig. 9, the cost comparison between full-bridge and flyback converters reveals an interesting insight. Despite the full-bridge converter showing higher efficiency, the overall cost of the flyback converter is significantly lower. In essence, while efficiency is undoubtedly a critical factor in converter selection, the general consideration of cost-effectiveness, proves the practical appeal and widespread utilization of flyback-based converters across various industrial sectors.

This cost advantage is a key reason why flyback converters are commonly preferred in various industrial applications. The simplicity of the flyback topology, requiring fewer components and offering straightforward implementation, contributes to its cost-effectiveness. This economic advantage makes flyback converters a widely adopted and practical solution in the industry for low power applications

A comprehensive evaluation has been conducted to compare the flyback-based converter [45] with the FB-based converter across various crucial parameters such as total voltage stress on primary switches, component count, volume, size, power density, full load efficiency, and cost. The detailed findings are summarized in Table 4, providing an insightful overview of the performance characteristics of the two converters. Fig. 10 further elucidates the comparison by presenting the specifications of the Flyback-based and FB-based prototypes. Upon careful examination of both the Table 5 and the graphical representation in Fig. 10, it becomes evident

levels, differing from light load to full load conditions. It is evident from this figure that the FB based converter exhibits a notably higher efficiency when compared to the flyback based converter. Fig. 8(b) and (c) present a detailed breakdown of losses within the power circuit for both converter types. The analysis reveals that the predominant source of losses in both converters is attributed to magnetic elements.
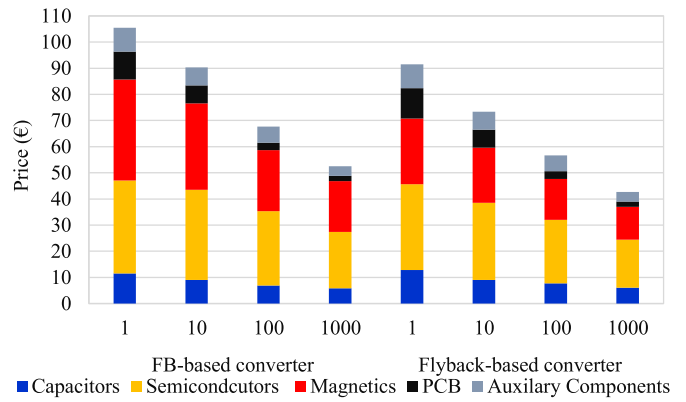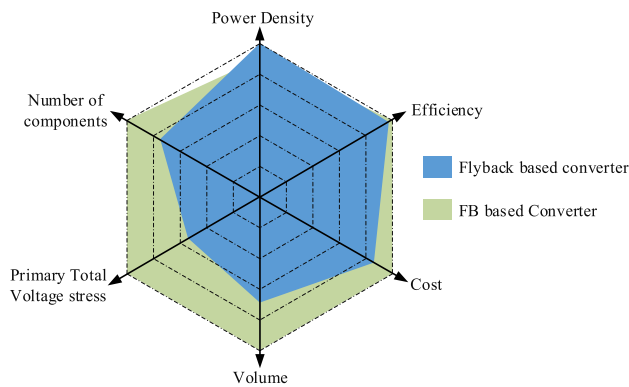
FIGURE. 10. The specification of the comparison between the Flyback based and FB based prototypes.

TABLE 5. Specification of the Two Converter Comparison

Topologies	Flyback based converter	FB Based Converter
Power Density	1.97 kw/dm^3	1.78 kw/dm^3
Efficiency	92.3 %	94.89 %
Cost	91 €	105 €
Volume	188*111*28 mm^3	165*111*46 mm^3
Total Voltage stress of primary side	197 V	360 V
Number of main components	9	12

that the flyback-based converter exhibits superiority in several aspects when compared to the FB-based converter. Despite the high efficiency of the FB-based converter, it is noteworthy that it incurs elevated costs and experiences increased total voltage stress across the switches, unlike the flyback-based counterpart. Notably, the flyback-based converter demonstrates a favorable combination of high power density and a reduced number of components, contributing to an overall cost reduction in the converter assembly.

In a comparative analysis between the flyback based converter and the FB based converter, it is initially observed that the flyback converter imposes a higher voltage stress on a switch than the FB counterpart. However, considering the number of switches, the overall voltage stress of the full-bridge converter surpasses that of the flyback converter. Additionally, alternative flyback converters, such as the one presented in [47], demonstrate parity in voltage stress with the full-bridge converter for individual switches.

Based on comprehensive theoretical analysis and the practical results showcased for converters within the transformer and coupled inductor family, it is evident that several key parameters must be considered for the effective deployment of these converters in industrial applications. These crucial parameters include, but are not limited to, the number of elements, efficiency, and notably the cost. In the realm of industrial applications, the selection of an appropriate converter structure demands a precise evaluation, taking into account the complicated balance between these fundamental criteria. Efficiency, cost-effectiveness, and the specific requirements

of the intended application all play fundamental roles in determining the optimal choice. This consideration is superior in achieving not only optimal performance but also cost-efficient and sustainable solutions for different industrial applications.

V. CONCLUSION

This paper presented a comprehensive evaluation of isolated high step-up dc-dc converters, emphasizing their applicability in distributed generation systems powered by renewable energy sources. The overview of competitive solutions highlights the importance of power electronic structures in incorporating renewable energy into the power grid, emphasizing their widespread and rapidly expanding usage. Through a comparative analysis, key parameters such as voltage conversion ratio, semiconductor element voltage stress, component size, and conduction and switching losses are considered. The selected configurations are also assessed in terms of cost estimation and financial feasibility. The investigation aims to guide researchers in identifying suitable isolated topologies with wide input voltage ranges and galvanic isolation for future research directions.

The comparison methodology is provided as systematic approach, considering capacitor and magnetic sizes, primary side switch voltage stress, primary side semiconductor conduction losses, and switching losses. The experimental examples of isolated dc-dc converters, specifically the flyback-based and full-bridge-based converters, validate the methodology and showcase distinct performance characteristics between the two.

The efficiency curve, losses breakdown, thermal characteristics, and cost comparison provide a comprehensive understanding of the trade-offs between the flyback and FB converters. Despite the higher efficiency of the FB converter, the cost-effectiveness of the flyback converter, attributed to its simplicity and fewer components, demonstrates its practical appeal in various industrial applications.

In conclusion, based on the comparative analysis and experimental validation, the paper recommends considering specific application requirements when choosing isolated high step-up dc-dc converters. The findings emphasize the importance of balancing efficiency and cost-effectiveness for practical implementation in distributed generation systems using renewable energy sources.

REFERENCES

[1] M. Malinowski, J. I. Leon, and H. Abu-Rub, "Solar photovoltaic and thermal energy systems: Current technology and future trends," *Proc. IEEE*, vol. 105, no. 11, pp. 2132–2146, Nov. 2017.

[2] J. Zeng, X. Du, and Z. Yang, "A multiport bidirectional DC–DC converter for hybrid renewable energy system integration," *IEEE Trans. Power Electron.*, vol. 36, no. 11, pp. 12281–12291, Nov. 2021.

[3] S. Gopinathan, V. S. Rao, and K. Sundaramoorthy, "Family of non-isolated quadratic high gain DC–DC converters based on extended capacitor-diode network for renewable energy source integration," *IEEE J. Emerg. Sel. Topics Power Electron.*, vol. 10, no. 5, pp. 6218–6230, Oct. 2022.

[4] Y. Yang et al., *Adv. in Grid-Connected Photovolt. Power Convers. Syst.*, Woodhead Publishing, 2018.

[5] H. Shayeghi, S. Pourjafar, M. Maalandish, and S. Nouri, "Non-isolated DC–DC converter with a high-voltage conversion ratio," *IET Power Electron.*, vol. 13, no. 16, pp. 3797–3806, Dec. 2020.

[6] E. L. Carvalho, A. Blinov, A. Chub, P. Emiliani, G. de Carne, and D. Vinnikov, "Grid integration of DC buildings: Standards, requirements and power converter topologies," *IEEE Open J. Power Electron.*, vol. 3, pp. 798–823, Oct. 2022.

[7] S. Beheshtaein, R. M. Cuzner, M. Forouzesh, M. Savaghebi, and J. M. Guerrero, "DC Microgrid protection: A comprehensive review," *IEEE J. Emerg. Sel. Topics Power Electron.*, early access, Mar. 12, 2019, doi: 10.1109/JESTPE.2019.2904588

[8] L. Mackay, N. H. van der Blij, L. Ramirez-Elizondo, and P. Bauer, "Toward the universal DC distribution system," *Electric Power Compon. Syst.*, vol. 45, no. 10, pp. 1032–1042, 2017.

[9] O. Matiushkin, O. Husev, D. Vinnikov, and J. Kurnitski, "DC-Ready photovoltaic solar converter," in *Proc.IEEE Int. Exhib. Conf. Power Electron., Intell. Motion, Renewable Energy Energy Manage.*, Nuremberg, Germany, 2023, pp. 1–7.

[10] P. Mohseni, S. Rahimpour, M. Dezhbord, M. R. Islam, and K. M. Muttaqi, "An optimal structure for high step-up non-isolated DC–DC converters with soft-switching capability and zero input current ripple," *IEEE Trans. Ind. Electron.*, vol. 69, no. 5, pp. 4676–4686, May 2022.

[11] S. Pourjafar, H. Shayeghi, S. M. Hashemzadeh, F. Sedaghati, and M. Maalandish, "A non-isolated high step-up DC–DC converter using magnetic coupling and voltage multiplier circuit," *IET Power Electron.*, vol. 14, no. 9, pp. 1637–1655, Jul. 2021.

[12] P. Alavi, P. Mohseni, E. Babaei, and V. Marzang, "An ultra-high step-up DC–DC converter with extendable voltage gain and soft-switching capability," *IEEE Trans. Ind. Electron.*, vol. 14, no. 9, pp. 4676–4686, May 2022.

[13] P. K. Maroti, S. Padmanaban, J. B. Holm-Nielsen, M. Sagar Bhaskar, M. Meraj, and A. Iqbal, "A new structure of high voltage gain SEPIC converter for renewable energy applications," *IEEE Access*, vol. 7, pp. 89857–89868, 2019.

[14] Y. Liu, W. Zhang, Y. Sun, M. Su, G. Xu, and H. Dan, "Review and comparison of control strategies in active power decoupling," *IEEE Trans. Power Electron.*, vol. 36, no. 12, pp. 14436–14455, Dec. 2021.

[15] O. Matiushkin, O. Husev, H. Afshari, D. Vinnikov, and R. Strzelecki, "Cost-effective piggyback forward based DC-DC converter," in *Proc. IEEE Appl. Power Electron. Conf. Expo.*, 2024, pp. 2106–2111.

[16] J. Yuan, F. Blaabjerg, Y. Yang, A. Sangwongwanich, and Y. Shen, "An overview of photovoltaic microinverters: Topology, efficiency, and reliability," in *Proc. IEEE 13th Int. Conf. Compat., Power Electron. Power Eng.*, 2019, pp. 1–6.

[17] M. Forouzesh, Y. P. Siwakoti, S. A. Gorji, F. Blaabjerg, and B. Lehman, "Step-up DC–DC converters: A comprehensive review of voltage-boosting techniques, topologies, and applications," *IEEE Trans. Power Electron.*, vol. 32, no. 12, pp. 9143–9178, Dec. 2017.

[18] Y. Koç, Y. Birbir, and H. Bodur, "Non-isolated high step-up DC-DC converters–An overview," *Alexandria Eng. J.*, vol. 61, no. 2, pp. 1091–1132, Feb. 2022.

[19] O. Husev, L. Liivik, F. Blaabjerg, A. Chub, D. Vinnikov, and I. Roasto, "Galvanically isolated quasi-z-source DC–DC converter with a novel ZVS and ZCS technique," *IEEE Trans. Ind. Electron.*, vol. 62, no. 12, pp. 7547–7556, Dec. 2015.

[20] E. S. Oluwasogo and H. Cha, "A quadratic quasi-z-source full-bridge isolated DC–DC converter with high reliability for wide input applications," *IEEE Trans. Ind. Electron.*, vol. 69, no. 10, pp. 10090–10100, Oct. 2022.

[21] J. Lee, M. Kim, S. Kim, and S. Choi, "An isolated single-switch ZCS resonant converter with high step-up ratio," *IEEE Trans. Power Electron.*, vol. 36, no. 10, pp. 11555–11564, Oct. 2021.

[22] N. Hassanpour, A. Chub, A. Blinov, and D. Vinnikov, "Soft-switching bidirectional step-up/down partial power converter with reduced components stress," *IEEE Trans. Power Electron.*, vol. 38, no. 11, pp. 14166–14177, Nov. 2023.

[23] Z. Zhang et al., "High efficiency step-up DC–DC converter for grid-connected photovoltaic microinverter applications," *IET Renewable Power Gener.*, vol. 16, no. 6, pp. 1159–1169, Apr. 2022.

[24] N. Yang, J. Zeng, R. Hu, and J. Liu, "Analysis and design of an isolated high step-up converter without voltage-drop," *IEEE Trans. Power Electron.*, vol. 37, no. 6, pp. 6939–6950, Jun. 2022.

[25] R. Kosenko, O. Husev, and A. Chub, "Full soft-switching high step-up current-fed DC-DC converters with reduced conduction losses," in *Proc. IEEE 5th Int. Conf. Power Eng., Energy Elect. Drives*, Riga, Latvia, 2015, pp. 170–175.

[26] M.-K. Nguyen, Y.-C. Lim, J.-H. Choi, and G.-B. Cho, "Isolated high step-up DC–DC converter based on quasi-switched-boost network," *IEEE Trans. Ind. Electron.*, vol. 63, no. 12, pp. 7553–7562, Dec. 2016.

[27] D. Vinnikov, J. Zakis, O. Husev, and R. Strzelecki, "New high-gain step-up DC/DC converter with high-frequency isolation," in *Proc. IEEE 27th Annu. Appl. Power Electron. Conf. Expo.*, Orlando, FL, USA, 2012, pp. 1204–1209.

[28] D. Vinnikov, A. Chub, O. Huse, and J. Zakis, "Quasi-Z-source half-bridge DC-DC converter for photovoltaic applications," in *Proc. IEEE Int. Conf. Ind. Technol.*, Seville, Spain, 2015, pp. 2935–2940.

[29] A. Chub, O. Husev, and D. Vinnikov, "Input-parallel output-series connection of isolated quasi-Z-source DC-DC converters," in *Proc. IEEE Electric Power Qual. Supply Rel. Conf.*, Rakvere, Estonia, 2014, pp. 277–284.

[30] A. Chub, D. Vinnikov, F. Blaabjerg, and F. Z. Peng, "A review of galvanically isolated impedance-source DC–DC converters," *IEEE Trans. Power Electron.*, vol. 31, no. 4, pp. 2808–2828, Apr. 2016.

[31] Y. C. Huang, Y. C. Hsieh, C. Y. Lin, and C. S. Moo, "Light load analysis and topology morphing between full/half-bridge DC-to-DC converter," *Int. J. Electron.*, vol. 111, pp. 298–317, 2023, doi: 10.1080/00207217.2022.2164070.

[32] H. Mao, S. Deng, J. Abu-Qahouq, and I. Batarseh, "Active-clamp snubbers for isolated half-bridge DC-DC converters," *IEEE Trans. Power Electron.*, vol. 20, no. 6, pp. 1294–1302, Nov. 2005.

[33] Q. Wu, Q. Wang, J. Xu, and Z. Xu, "Active-clamped ZVS current-fed push–pull isolated DC-DC converter for renewable energy conversion applications," *IET Power Electron.*, vol. 11, no. 2, pp. 373–381, Feb. 2018.

[34] Q. Wu, Q. Wang, J. Xu, and L. Xiao, "A wide load range ZVS push–pull DC-DC converter with active clamped," *IEEE Trans. Power Electron.*, vol. 32, no. 4, pp. 2865–2875, Apr. 2017.

[35] H. Kim, C. Yoon, and S. Choi, "An improved current-fed ZVS isolated boost converter for fuel cell applications," *IEEE Trans. Power Electron.*, vol. 25, no. 9, pp. 2357–2364, Sep. 2010.

[36] K. Kanathipan, R. Emamalipour, and J. Lam, "A single-switch high-gain PV microconverter with low-switch-voltage-to-high-voltage-bus ratio," *IEEE Trans. Power Electron.*, vol. 35, no. 9, pp. 9530–9540, Sep. 2020.

[37] A. R. Paul, A. Bhattacharya, and K. Chatterjee, "A novel SEPIC-ĆUK-based high gain solar PV microinverter for grid integration," *IEEE Trans. Ind. Electron.*, vol. 70, no. 12, pp. 12365–12375, Dec. 2023.

[38] A. Shawky, T. Takeshita, and M. A. Sayed, "Analysis and performance evaluation of single-stage three-phase SEPIC differential inverter with continuous input current for PV grid-connected applications," in *Proc. IEEE Appl. Power Electron. Conf. Expo.*, Phoenix, AZ, USA, 2021, pp. 2719–2726.

[39] S. A. Ansari and J. S. Moghani, "A novel high voltage gain noncoupled inductor SEPIC converter," *IEEE Trans. Ind. Electron.*, vol. 66, no. 9, pp. 7099–7108, Sep. 2019.

[40] N. Falconar, D. S. Beyragh, and M. Pahlevani, "An adaptive sensorless control technique for a flyback-type solar tile microinverter," *IEEE Trans. Power Electron.*, vol. 35, no. 12, pp. 13554–13562, Dec. 2020.

[41] R. Za'im, J. Jamaludin, and N. A. Rahim, "Photovoltaic flyback microinverter with tertiary winding current sensing," *IEEE Trans. Power Electron.*, vol. 34, no. 8, pp. 7588–7602, Aug. 2019.

[42] F. Zhang, Y. Xie, Y. Hu, G. Chen, and X. Wang, "A hybrid boost–flyback/flyback microinverter for photovoltaic applications," *IEEE Trans. Ind. Electron.*, vol. 67, no. 1, pp. 308–318, Jan. 2020.

[43] R. Erickson, M. Madigan, and S. Singer, "Design of a simple high-power-factor rectifier based on the flyback converter," in *Proc. IEEE 5th Annu. Proc. Appl. Power Electron. Conf. Expo.*, Los Angeles, CA, USA, Mar. 1990, pp. 792-801.

[44] B. Tamyurek and B. Kirimer, "An interleaved high-power flyback inverter for photovoltaic applications," *IEEE Trans. Power Electron.*, vol. 30, no. 6, pp. 3228–3241, Jun. 2015.

[45] H. Afshari, O. Husev, D. Vinnikov, O. Matiushkin, and N. V. Kurdkandi, "Comparison of grid-connected flyback-based microinverter with primary and secondary side decoupling approach," in *Proc. IEEE 63th Int. Sci. Conf. Power Elect. Eng. Riga Tech. Univ. (RTUCON)*, Riga, Latvia, 2022, pp. 1–6.

[46] I. Alhurayyis, A. Elkhateb, and J. Morrow, "Isolated and non-isolated DC-to-DC converters for medium-voltage dc networks: A review," *IEEE J. Emerg. Sel. Topics Power Electron.*, vol. 9, no. 6, pp. 7486–7500, Dec. 2021.

[47] W. Li, J. Liu, J. Wu, and X. He, "Design and analysis of isolated ZVT boost converters for high-efficiency and high-step-up applications," *IEEE Trans. Power Electron.*, vol. 22, no. 6, pp. 2363–2374, Nov. 2007.

[48] J.-Y. Lin, S.-Y. Lee, C.-Y. Ting, and F.-C. Syu, "Active-clamp forward converter with lossless-snubber on secondary-side," *IEEE Trans. Power Electron.*, vol. 34, no. 8, pp. 7650–7661, Aug. 2019.

[49] H. Wu and Y. Xing, "A family of forward converters with inherent demagnetizing features based on basic forward cells," *IEEE Trans. Power Electron.*, vol. 25, no. 11, pp. 2828–2834, Nov. 2010.

[50] H. Wu and Y. Xing, "Families of forward converters suitable for wide input voltage range applications," *IEEE Trans. Power Electron.*, vol. 29, no. 11, pp. 6006–6017, Nov. 2014.

[51] A. Abramovitz, T. Cheng, and K. Smedley, "Analysis and design of forward converter with energy regenerative snubber," *IEEE Trans. Power Electron.*, vol. 25, no. 3, pp. 667–676, Mar. 2010.

[52] T. Qian and Q. Wu, "A boost type resonant forward converter with topology combination," *IEEE Trans. Circuits Syst. II: Exp. Briefs*, vol. 65, no. 12, pp. 2008–2011, Dec. 2018.

[53] H. Afshari, O. Husev, and D. Vinnikov, "A novel isolated buck-boost DC-DC converter with wide range of voltage regulations," in *Proc. IEEE 17th Int. Conf. Compat., Power Electron. Power Eng.*, Tallinn, Estonia, 2023, pp. 1–6.

[54] Q. Wu, Q. Wang, J. Xu, H. Li, and L. Xiao, "A high-efficiency step-up current-fed push–pull quasi-resonant converter with fewer components for fuel cell application," *IEEE Trans. Ind. Electron.*, vol. 64, no. 8, pp. 6639–6648, Aug. 2017.

[55] T. Meghdad, M. Jafar, and A. Bijan, "High step-up current-fed ZVS dual half-bridge DC–DC converter for high-voltage applications," *IET Power Electron.*, vol. 8, no. 2, pp. 309–318, Feb. 2015.

[56] H.-S. Lee and J.-J. Yun, "Quasi-resonant voltage doubler with snubber capacitor for boost half-bridge DC–DC converter in photovoltaic micro-inverter," *IEEE Trans. Power Electron.*, vol. 34, no. 9, pp. 8377–8388, Sep. 2019.

[57] Z. Yao and J. Xu, "An improved integrated boost full-bridge converter," in *Proc. IEEE Smart Energy Grid Eng.*, Oshawa, ON, Canada, 2016, pp. 191–195.

[58] S. Pourjafar, P. Mohseni, O. Husev, O. Matiushkin, and D. Vinnikov, "Novel isolated high step-up DC-DC converter with wide input voltage regulation range," in *Proc. IEEE 64th Int. Sci. Conf. Power Elect. Eng. Riga Tech. Univ.*, 2023, pp. 1–6.

[59] K. Akbariavaz, S. S. Fazel, and M. Khosravi, "Fully FPGA-based implementation of a modified control strategy for power electronic transformer in railway traction applications," *IET Renewable Power Gener*, vol. 17, pp. 1904–1919, Apr. 2021.

[60] S. Deshmukh Gore et al., "Review on classification of resonant converters for electric vehicle application," *Energy Rep.*, vol. 8, pp. 1091–1113, Nov. 2022.

[61] Z. Yasser Yousefi and F. Seyed Saeed, "Soft-switching buck/boost full-bridge three-port converter for DC-DC applications," *Eng. Sci. Technol., an Int. J.*, vol. 41, May 2023, Art. no. 101382.

[62] R. Takarli, M. Adib, A. Vahedi, and R. Beiranvand, "A bidirectional CLLC resonant converter for EV battery charger applications," in *Proc. 14th Power Electron., Drive Syst., Technol. Conf.*, Babol, Iran, Islamic Republic of, 2023, pp. 1–6.

[63] M. Rezayati, F. Tahami, J. L. Schanen, and B. Sarrazin, "Generalized state-plane analysis of bidirectional CLLC resonant converter," *IEEE Trans. Power Electron.*, vol. 37, no. 5, pp. 5773–5785, May 2022.

[64] P. He, A. Mallik, A. Sankar, and A. Khaligh, "Design of a 1-MHz high-efficiency high-power-density bidirectional GaN-based CLLC converter for electric vehicles," *IEEE Trans. Veh. Technol.*, vol. 68, no. 1, pp. 213–223, Jan. 2019.

[65] Y. Wei, Q. Luo, and H. A. Mantooth, "A resonant frequency tracking technique for LLC converter-based DC transformers," *IEEE J. Emerg. Sel. Topics Ind. Electron.*, vol. 2, no. 4, pp. 579–590, Oct. 2021.

[66] S. Tandon and A. K. Rathore, "Analysis and design of series LC resonance-pulse based zero-current-switching current-fed half-bridge DC–DC converter," *IEEE Trans. Ind. Electron.*, vol. 68, no. 8, pp. 6784–6793, Aug. 2021.

[67] H. Seok, B. Han, B.-H. Kwon, and M. Kim, "High step-up resonant DC–DC converter with ripple-free input current for renewable energy systems," *IEEE Trans. Ind. Electron.*, vol. 65, no. 11, pp. 8543–8552, Nov. 2018.

[68] D. Menzi, D. Bortis, and J. W. Kolar, "A new bidirectional three-phase phase-modular boost-buck AC/DC converter," in *Proc. IEEE Int. Power Electron. Application Conf. Expo.*, 2018, pp. 1–8.

[69] O. Husev, O. Matiushkin, T. Jalakas, D. Vinnikov, and N. V. Kurd-kandi, "Comparative evaluation of dual-purpose converters suitable for application in DC and AC grids," *IEEE J. Emerg. Sel. Topics Power Electron.*, vol. 12, no. 2, pp. 1337–1347, Apr. 2024.

[70] O. Husev et al., "Comparison of impedance-source networks for two and multilevel buck–boost inverter applications," *IEEE Trans. Power Electron.*, vol. 31, no. 11, pp. 7564–7579, Nov. 2016.

[71] H. Tarzamni, H. S. Gohari, M. Sabahi, and J. Kyyrä, "Non-isolated high step-up DC–DC converters: Comparative review and metrics applicability," *IEEE Trans. Power Electron.*, vol. 39, no. 1, pp. 582–625, Jan. 2024.

[72] B. Andres, L. Romitti, F. H. Dupont, L. Roggia, and L. Schuch, "A high step-up isolated DC–DC converter based on voltage multiplier cell," *Int. J. Circuit Theory Appl.*, vol. 51, no. 2, pp. 557–578, Feb. 2023.

[73] D. Sha, X. Wang, and D. Chen, "High-efficiency current-fed dual active bridge DC–DC converter with ZVS achievement throughout full range of load using optimized switching patterns," *IEEE Trans. Power Electron.*, vol. 33, no. 2, pp. 1347–1357, Feb. 2018.

[74] M. A. Chewale, R. A.Wanjari, V. B.Savakhande, and P. R.Sonawane, "A review on isolated and non-isolated DC-DC converter for PV application," in *Proc. Int. Conf. Control, Power, Commun. Comput. Technol.*, Kannur, India, 2018, pp. 399–404.

SAEED POURJAFAR (Member, IEEE) was born in Ardabil, Iran. He received the B.Sc. degree in electrical engineering from Azerbaijan Shahid Madani University, Tabriz, Iran, in 2015, and the M.Sc. degree in power electronics and drives from the Faculty of Electrical and Computer Engineering, Sahand University of Technology, Tabriz, in 2017, and the Ph.D. degree in power electronics and drives with the Energy Management Research Center, University of Mohaghegh Ardabili, Ardabil, Iran, in 2021. He is currently a Postdoctoral researcher with the Tallinn University of Technology, Tallinn, Estonia, focusing on dc-dc converters and the application of power electronics in renewable systems.

HOSSEIN AFSHARI (Student Member, IEEE) received the master's degree in electrical engineering from the Iran University of Science & Technology, Tehran, Iran. He has worked in the area of Power Electronics especially on Power Electronic Converters, DC-DC converters, as well as switching power supplies and also microconverters. Since May 2022, he has been the researcher with the Tallinn University of Technology, Tallinn, Estonia.

PARHAM MOHSENI (Student Member, IEEE) received the M.Sc. degree in power electronics and electrical machines from the University of Tabriz, Tabriz, Iran, in 2017. He is currently working toward the Ph.D. degree in electrical power engineering and mechatronics with Tallinn University of Technology, Tallinn, Estonia. His research interests include high-step-up power electronic converters, soft-switching circuits, multiple-input/output converters, and onboard chargers.

OLEKSANDR HUSEV (Senior Member, IEEE) received the Ph.D. degree from the Institute of Electrodynamics, National Academy of Science of Ukraine, Kyiv, Ukraine, in 2012. He currently a Senior Researcher and project Leader with the Department of Electrical Power Engineering and Mechatronics, Tallinn University of Technology, Tallinn, Estonia. His research interests include power electronics systems, novel topology design, control systems employing various algorithms, modeling, simulation, and applied power converter.

NOMAN SHABBIR (Senior Member, IEEE) received the B.S. degree in computer engineering from COMSATS University, Lahore, Pakistan, the M.S. degree in electrical engineering from the Blekinge Institute of Technology, Karlskrona, Sweden, and the Ph.D. degree in electrical power engineering and mechatronics from TalTech Estonia, Tallinn, Estonia, in 2022. He is currently a Research Fellow with the FinEST Center for smart cities, Tallinn, Estonia. His research interests include renewable energy systems, energy management, energy flexibility, and AI applications in Energy systems.

OLEKSANDR MATIUSHKIN (Member, IEEE) received the B.Sc. and M.Sc. degrees in industrial electronics from the Chernihiv National University of Technology, Chernihiv, Ukraine, in 2016 and 2018, respectively, and the Ph.D. degree in power electronics from the Tallinn University of Technology, Tallinn, Estonia, in 2022. He is currently a researcher with the Department of Electrical Engineering, Tallinn University of Technology. His research interests include power electronics, new topology design, microcontroller and FPGA programming, modeling, filter calculations, and control techniques for power electronics converters.